Lupus-like autoimmune disease caused by a lack of Xkr8, a caspase-dependent phospholipid scramblase

Mahiru Kawano[a] and Shigekazu Nagata[a,1]

[a]Laboratory of Biochemistry and Immunology, World Premier International Immunology Frontier Research Center, Osaka University, Suita, 565-0871 Osaka, Japan

Contributed by Shigekazu Nagata, January 19, 2018 (sent for review November 28, 2017; reviewed by Rikinari Hanayama and Kirsten Lauber)

Apoptotic cells expose phosphatidylserine (PtdSer) on their cell surface and are recognized by macrophages for clearance. Xkr8 is a scramblase that exposes PtdSer in a caspase-dependent manner. Here, we found that among the three Xkr members with caspase-dependent scramblase activity, mouse hematopoietic cells express only Xkr8. The PtdSer exposure of apoptotic thymocytes, splenocytes, and neutrophils was strongly reduced when Xkr8 was absent. While wild-type apoptotic lymphocytes and neutrophils were efficiently engulfed in vitro by phagocytes expressing Tim4 and MerTK, *Xkr8*-deficient apoptotic cells were hardly engulfed by these phagocytes. Accordingly, the number of apoptotic thymocytes in the thymus and neutrophils in the peritoneal cavity of the zymosan-treated mice was significantly increased in *Xkr8*-deficient mice. The percentage of CD62L^{lo} senescent neutrophils was increased in the spleen of *Xkr8*-null mice, especially after the treatment with granulocyte colony-stimulating factor. *Xkr8*-null mice on an MRL background showed high levels of autoantibodies, splenomegaly with high levels of effector CD4 T cells, and glomerulonephritis development with immune-complex deposition at glomeruli. These results indicate that the Xkr8-mediated PtdSer exposure in apoptotic lymphocytes and aged neutrophils is essential for their clearance, and its defect activates the immune system, leading to lupus-like autoimmune disease.

efferocytosis | macrophages | neutrophils | scramblase | senescence

During animal development, many unnecessary or toxic cells die (1). In animals after birth, large numbers of senescent cells, and cells infected by viruses and bacteria, die or are killed by cytotoxic cells. Among several programmed cell death processes (apoptosis, necroptosis, and pyroptosis), apoptosis is important in the physiological cell death during animal development. In apoptosis, various molecules activate a cascade of caspases, the last of which is caspase 3, and cleaves more than 400 cellular substrates, manifesting the hallmarks of apoptosis such as DNA fragmentation, membrane blebbing, and cell shrinkage (2). The apoptotic pathway is used to block necroptosis, and its defect causes abnormal cell accumulation or tissue necrosis, depending on the step at which the apoptosis is blocked (3).

Apoptotic cells are swiftly recognized and engulfed by macrophages before their plasma membrane is ruptured, to prevent the release of intracellular materials that may activate the immune system (4–6). Macrophages engulf apoptotic cells but not living cells, which led to the proposal that apoptotic cells expose an "eat me" signal (7). The process of apoptotic-cell engulfment is called "efferocytosis," and phosphatidylserine (PtdSer) is the strongest candidate for the eat me signal (5, 8). PtdSer is an abundant phospholipid in the plasma membrane, where it is confined to the inner leaflet by the action of flippases that translocate PtdSer and phosphatidylethanolamine from the outer leaflet (9, 10). We recently identified two P4-type ATPases (ATP11A and ATP11C) that are ubiquitously expressed in the plasma membrane as the flippase (11, 12). These flippases contain caspase-recognition sites in the middle of the molecule and are inactivated by caspase during apoptosis. This caspase-mediated flippase inactivation is necessary but not sufficient for the apoptotic PtdSer exposure (5).

To quickly expose PtdSer on the surface of apoptotic cells, a scramblase that nonspecifically and bidirectionally translocates phospholipids between the inner and outer membrane leaflets has been postulated (9). We previously identified three Xkr members (Xkr4, Xkr8, and Xkr9) as scramblases that are activated in apoptotic cells. These molecules are membrane proteins with 10 transmembrane regions, and carry a caspase-recognition site in their C-terminal region (13, 14). The cleavage of Xkr8 by caspase 3 induces a conformational change that turns on its scramblase activity (15).

In this study, we found that mouse hematopoietic cells express only Xkr8 among the three Xkr members with caspase-dependent scramblase activity. The PtdSer exposure of apoptotic thymocytes, splenocytes, and neutrophils was strongly delayed by *Xkr8* deficiency. Accordingly, the efferocytosis of these cells was retarded. We also found that the percentage of senescent CD62L^{lo} neutrophils in the spleen increased in *Xkr8*$^{-/-}$ mice. The *Xkr8*-null mice developed autoantibodies [anti-DNA and antinuclear antibodies (ANA)], and suffered from glomerular nephritis. These results indicate that the Xkr8-mediated PtdSer exposure in apoptotic lymphocytes and senescent neutrophils, followed by their engulfment, is a critical step in apoptosis that prevents the release of noxious materials from dying or senescent cells.

Results

Specific Expression of Xkr8 in Mouse Hematopoietic Cells. We previously reported that mouse thymus and spleen express Xkr8, Xkr4, and Xkr9 (13, 14). Here we found by real-time RT-PCR that a substantial level of Xkr4 as well as Xkr9 mRNA was present in the thymus and spleen (Fig. S1). In contrast, cells in the bone marrow (13, 14) and mononuclear leukocytes in the

Significance

Every day in our bodies, billions of neutrophils become senescent and are cleared by macrophages. This number exceeds the number of cells that undergo apoptosis. Xkr8 is a member of the Xkr membrane-protein family and has caspase-dependent phospholipid scramblase activity. Here, we show that not only apoptotic thymocytes and splenocytes, but also senescent neutrophils require Xkr8 for swift clearance in vivo. *Xkr8*-deficient female mice on the MRL background carried high levels of autoantibodies, accumulated effector CD4 T cells, and developed glomerulonephritis. These results indicate that in addition to unengulfed apoptotic cells, uncleared senescent neutrophils contribute to the development of autoimmune diseases.

Author contributions: M.K. and S.N. designed research; M.K. performed research; M.K. analyzed data; and M.K. and S.N. wrote the paper.

Reviewers: R.H., Kanazawa University Graduate School of Medical Sciences; and K.L., University Hospital, Ludwig Maximilian University.

The authors declare no conflict of interest.

[1]To whom correspondence should be addressed. Email: snagata@ifrec.osaka-u.ac.jp.

This article contains supporting information online at www.pnas.org/lookup/suppl/doi:10.1073/pnas.1720732115/-/DCSupplemental.

Published online February 12, 2018.

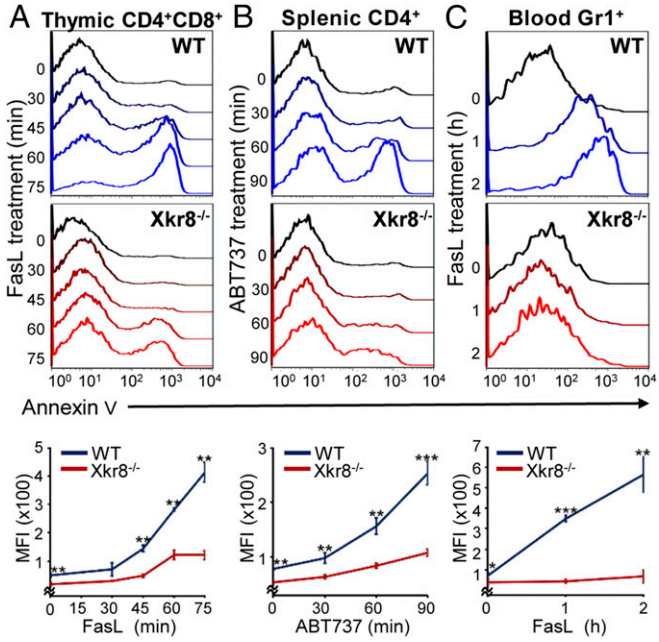

Fig. 1. *Xkr8*-null mutation decreases apoptotic PtdSer exposure. Thymocytes (*A*), splenocytes (*B*), and peripheral blood mononuclear cells (*C*) from 6- to 8-wk-old wild-type (WT) or *Xkr8*$^{-/-}$ C57BL/6 mice were treated at 37 °C for the indicated periods with 100 units/mL FasL (*A* and *C*) or 10 μM ABT737 (*B*). The cells were stained with Cy5-annexin V and Sytox blue, together with PE-anti-CD3, FITC-anti-CD4, PE/Cy7-anti-CD8, or PE-anti-Gr1, and analyzed by flow cytometry. The annexin V-staining profiles for CD4$^+$CD8$^+$ thymocytes (*A*), CD4$^+$ splenocytes (*B*), and Gr1$^+$ neutrophils (*C*) in the Sytox Blue-negative population at the indicated times are shown. The experiments were carried out independently three times, and the mean fluorescent intensity (MFI) was plotted with SD (bar) at *Bottom*. **P* < 0.05, ***P* < 0.01, ****P* < 0.001, two-sided Student's *t* test.

blood expressed only Xkr8. Since the thymus and spleen consist of not only lymphocytes but also stromal cells, we suspected that the Xkr4 or Xkr9 mRNA was expressed in stromal cells, but not in lymphocytes. In fact, thymocytes and lymphocytes expressed a high level of Xkr8 mRNA, but neither Xkr4 nor Xkr9 mRNA (Fig. S1).

Xkr8-Dependent Apoptotic PtdSer Exposure and Cell Engulfment by Phagocytes. To examine the requirement of primary mouse hematopoietic cells for Xkr8 to expose PtdSer during apoptosis, thymocytes and neutrophils were treated with Fas ligand (FasL), while splenocytes were treated with ABT737, a BH3 mimetic that activates the mitochondrial apoptosis pathway (16). As shown in Fig. 1*A*, the wild-type CD4$^+$CD8$^+$ thymocytes quickly exposed PtdSer upon FasL treatment (within 75 min), while the FasL-induced PtdSer exposure was severely retarded in *Xkr8*$^{-/-}$ thymocytes. Similar Xkr8-dependent PtdSer exposure was observed in ABT737-treated splenic CD4$^+$ T cells (Fig. 1*B*) and FasL-treated blood Gr1$^+$ neutrophils (Fig. 1*C*).

PtdSer-exposing apoptotic cells are engulfed by phagocytes in a PtdSer-dependent manner (5). We recently showed that resident peritoneal macrophages and Kupffer cells engulf apoptotic cells via a PtdSer-receptor Tim4 and a TAM family receptor (17). The ability of these macrophages to perform efferocytosis can be recapitulated using an NIH 3T3-derivative expressing Tim4 and MerTK (TKO-Tim4/Mer) (17). To examine the effect of the *Xkr8*-null mutation on efferocytosis, thymocytes, CD3$^+$ splenocytes, and blood neutrophils were labeled with pHrodo, treated with an apoptosis inducer, and added to TKO-Tim4/Mer cells at a ratio of 1:2–1:5 (phagocytes:prey). As shown in Fig. 2, the wild-type apoptotic cells were engulfed within 45–60 min, and many pHrodo-positive dead cells were found inside the phagocytes. On the other hand, 65–94% fewer pHrodo-positive dead cells were found in the phagocytes when *Xkr8*$^{-/-}$ cells were used as prey. These results indicated that the Xkr8-mediated PtdSer exposure is essential for efficient efferocytosis.

Effect of Xkr8 on the Clearance of Apoptotic Thymocytes in Vivo. In the thymus, many T cells are eliminated by apoptosis (18). TUNEL staining (19) of the thymus of 5-wk-old wild-type mice for apoptotic cells revealed that about 0.6% of the thymocytes scattered in the cortex were TUNEL positive (Fig. 3*A* and Fig. S2). More than 90% TUNEL-positive cells were associated with CD68$^+$ macrophages, confirming that the apoptotic cells were quickly engulfed by macrophages (18). The thymus of *Xkr8*-null mice contained twice as many TUNEL-positive cells (1.3%), and the percentage of the TUNEL-positive cells that were not associated with macrophages significantly increased, suggesting that the efferocytosis of *Xkr8*$^{-/-}$ thymocytes was retarded.

Treating mice with dexamethasone causes massive apoptosis of thymocytes that are cleared by macrophages in the thymus (18). At 12 h after dexamethasone treatment, 60% more TUNEL-positive cells were observed in the thymic cortex of *Xkr8*$^{-/-}$ mice than in that of wild-type mice (Fig. 3*B*). Since the sensitivity to dexamethasone-induced apoptosis was similar between the wild-type and *Xkr8*$^{-/-}$

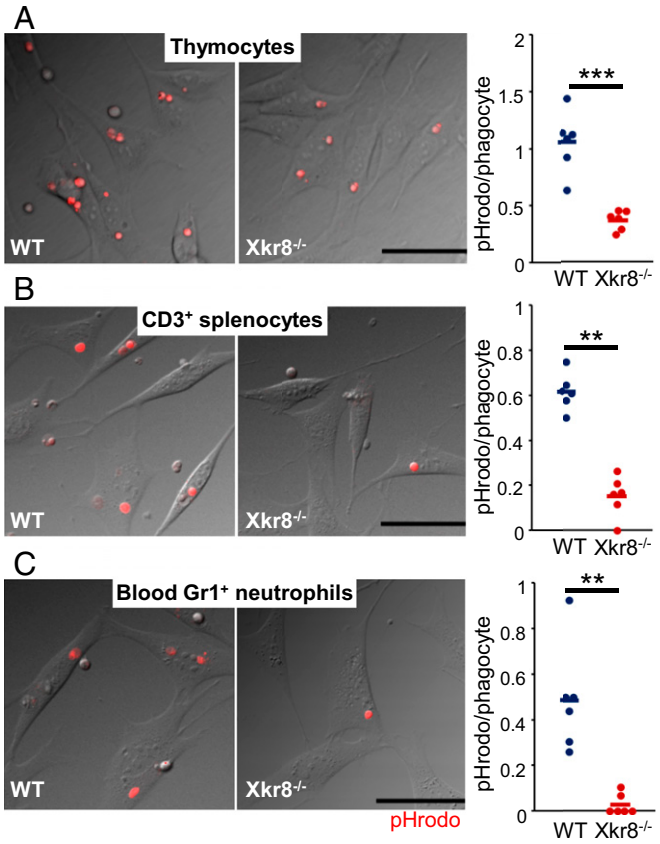

Fig. 2. *Xkr8*-null mutation decreases efferocytosis in vitro. Thymocytes (*A*), CD3$^+$ splenocytes (*B*), or blood Gr1$^+$ neutrophils (*C*) from 6- to 9-wk-old wild-type (WT) or *Xkr8*$^{-/-}$ C57BL/6 mice were labeled with pHrodo, and treated at 37 °C with 100 units/mL FasL for 30 min (*A*) or 60 min (*C*), or with 10 μM ABT737 for 30 min (*B*). The apoptotic cells were then incubated at 37 °C with TKO-Tim4/Mer cells at a (phagocyte:prey) ratio of 1:2 (*A*), 1:5 (*B*), or 1:2.5 (*C*), for 45 min (*A*) or 60 min (*B* and *C*), and observed by fluorescence microscopy. (Scale bar, 50 μm.) In *Right* panels, the number of pH-positive engulfed cells (red) was counted in six different fields (150–200 total phagocytes), and expressed as a ratio to the number of phagocytes. The experiments were carried out three times. Bar indicates the average value. ***P* < 0.01, ****P* < 0.001; two-sided Student's *t* test.

CELL BIOLOGY

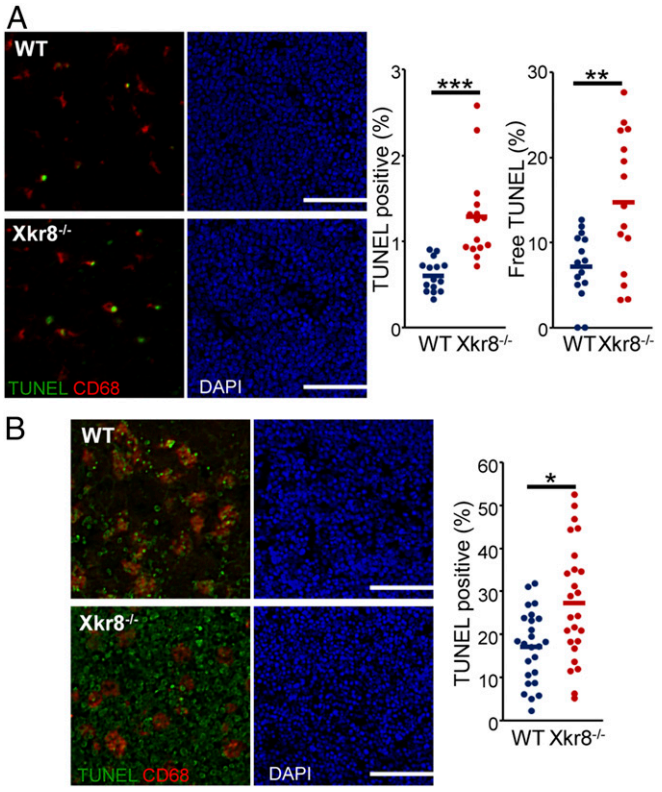

Fig. 3. *Xkr8*-null mutation decreases the clearance of apoptotic thymocytes in vivo. (*A*) Effect of the *Xkr8*-null mutation on TUNEL-positive thymocytes. Cryosections of the thymic cortex from 5-wk-old wild-type (WT) and *Xkr8*$^{-/-}$ C57BL/6 mice (n = 3 for each) were stained for TUNEL and CD68, counterstained with DAPI, and observed by fluorescence microscopy. In *Right* panels, the area of TUNEL-positive spots was quantified in five fields and expressed as a ratio to the DAPI-positive area. Bar indicates the average value. The TUNEL-positive spots that were not associated with CD68^{+} area were also quantified and expressed as percentage of the TUNEL-positive area. (*B*) Six- to 8-wk-old wild-type or *Xkr8*$^{-/-}$ C57BL/6 (n = 5 for each) were i.p. injected with dexamethasone. Twelve hours later, cryosections of the thymic cortex were stained for TUNEL and CD68. At *Right*, the area of TUNEL-positive spots was quantified and expressed as above. *P < 0.05, **P < 0.01, ***P < 0.001; two-sided Student's t test. (Scale bar, 50 μm.)

thymocytes (Fig. S3), these results suggested that the clearance of dexamethasone-induced apoptotic thymocytes was delayed in the absence of Xkr8.

Effect of Xkr8 on the Clearance of Neutrophils in Vivo. The in vivo effect of the Xkr8-mediated PtdSer exposure in the clearance of apoptotic neutrophils was examined with zymosan-induced peritonitis, in which a large number of neutrophils are infiltrated into the peritoneal cavity and undergo apoptosis (20, 21). These apoptotic neutrophils are cleared by the macrophages that were subsequently recruited into the peritoneal cavity. As shown in Fig. 4*A*, at 18 h after the injection of zymosan, the number of neutrophils in the cavity was 3.6×10^6 and 7.2×10^6 cells in the wild-type and *Xkr8*$^{-/-}$ mice, respectively, indicating that the apoptotic neutrophils generated during peritonitis were not efficiently cleared without Xkr8.

We then examined the effect of Xkr8 on the clearance of senescent neutrophils. Since senescent neutrophils down-regulate CD62L (L-selectin), they can be recognized as a CD62L^{lo} population (22). The number of CD62L^{lo}Gr1^{+} cells in the blood was similar between wild-type and *Xkr8*$^{-/-}$ mice at the age of 7 wk. Senescent neutrophils are cleared in the liver, spleen, and bone marrow (23). The number of Gr1^{+} neutrophils in the spleen of *Xkr8*$^{-/-}$ mice was comparable to that in wild-type spleen. Staining of the Gr1^{+} neutrophils for CD62L revealed two populations, and CD62L^{lo} but not CD62L^{hi} cells contained caspase 3/7-positive cells (Fig. 4*B*). The CD62L^{lo} population increased by about 21% in the *Xkr8*$^{-/-}$ mice. The percentage of the caspase 3/7-positive cells in CD62L^{lo} neutrophils also increased from 5.5 to 7.6%, supporting the idea that the senescent neutrophils underwent apoptosis and were engulfed by macrophages in a Xkr8-dependent manner. To confirm the requirement of Xkr8 in the clearance of CD62L^{lo} senescent neutrophils, mice were treated with granulocyte colony-stimulating factor (G-CSF) once a day for 3 d. This treatment increased the number of blood neutrophils from 1×10^6/mL to 5×10^6/mL in both the wild-type and *Xkr8*$^{-/-}$ mice. Ten hours after the last injection of G-CSF, the percentage of neutrophils in the spleen was higher by 70% in the *Xkr8*$^{-/-}$ mice than in the wild-type mice. This increase in the number of neutrophils in the spleen of *Xkr8*$^{-/-}$ mice was accompanied by an increase in the CD62L^{lo} neutrophils from 42% to 65% (Fig. 4*B*).

Elevation of Autoantibodies and Glomerulonephritis in *Xkr8*$^{-/-}$ Mice. The deficiency in clearing apoptotic cells and senescent neutrophils suggested that the *Xkr8*$^{-/-}$ mice might develop a lupus-like phenotype, but the C57BL/6-*Xkr8*$^{-/-}$ mice did not develop autoimmunity. Since the MRL mouse strain has an exaggerated response to low-affinity antigens for developing autoimmunity compared with C57BL/6 mice (24), the *Xkr8*$^{-/-}$ locus was transferred to the MRL strain using speed congenics. After dexamethasone treatment, as found with the C57BL/6 strain, the MRL mice with the *Xkr8*-null mutation had a defect in clearing apoptotic thymocytes (Fig. S4). Like MRL-*lpr* mice, which lack Fas, the female MRL-*Xkr8*$^{-/-}$ mice developed splenomegaly in an age-dependent manner. The size of the spleen of 50-wk-old *Xkr8*-deficient mice was approximately twice that of the wild-type MRL mice (Fig. 5*A*). About 78% of the CD4^{+} T cells in the spleen of MRL-*Xkr8*$^{-/-}$ mice appeared to be activated with a CD44^{hi} CD62L^{lo} cell-surface phenotype, which was much higher than that found in the wild-type MRL mice (27% of CD4^{+} T cells) (Fig. 5*B*). This high percentage of activated T cells in the MRL-*Xkr8*$^{-/-}$ mice was comparable to or higher than that observed in MRL-*lpr* mice (25). The levels of ANAs and anti-dsDNA antibodies in the serum of 40-wk-old female MRL-*Xkr8*$^{-/-}$ mice were two to three times those in the wild-type littermate serum (Fig. 5*C*), indicating that B cells against autoantigens were activated by the *Xkr8* deficiency. Circulating autoantibodies are known to cause immune-complex deposition in the glomeruli of the kidney. Notably, the glomeruli in 50-wk-old female MRL-*Xkr8*$^{-/-}$ mice showed substantial IgG deposition (Fig. 5*D*). This deposition was accompanied by the enlargement and hypercellularity of the glomeruli in about 60% of these mice.

Discussion

The XKR family has nine and eight members in humans and mice, respectively (26), three of which (Xk4, Xkr8, and Xkr9) have caspase-dependent scramblase activity (14). We found that although both Xkr4 and Xkr8 mRNAs were present in the mouse spleen and thymus, the thymocytes and splenocytes expressed only Xkr8. Xkr8 is also expressed in embryonal fibroblasts and hepatocytes (13), indicating that Xkr8 is broadly expressed in various cell types, while Xkr4 and Xkr9 are expressed in a cell type-specific manner. The genes of XKR family members are scattered on various chromosomes, and the promoter sequences of Xkr4, Xkr8, and Xkr9 have no apparent similarity. Like the human Xkr8 gene (13), the promoter region of the mouse Xkr8 gene is rich in CpG motifs and has several Sp1-binding sites, which is a characteristic of housekeeping genes. Cells in the brain and intestine express Xkr4 or Xkr9 in addition to the ubiquitous Xkr8. Whether different cell populations in these tissues use Xkr4, Xkr8, or Xkr9 for their caspase-dependent scramblase activity remains to be investigated.

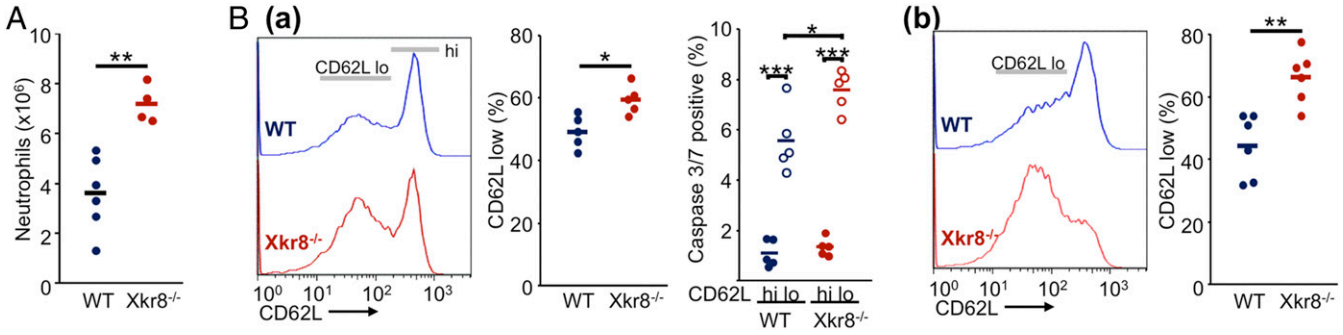

Fig. 4. *Xkr8*-null mutation decreases the clearance of neutrophils in vivo. (*A*) Effect of the *Xkr8*-null mutation on clearance of neutrophils in peritonitis. The 6- to 8-wk-old wild-type ($n = 6$) or *Xkr8*$^{-/-}$ ($n = 4$) C57BL/6 were i.p. injected with zymosan. Eighteen hours later, the cells in the peritoneal cavity were collected, and the number of Gr1^{+} neutrophils was plotted with the average value (bar). (*B*) Effect of the *Xkr8*-null mutation on the clearance of CD62L^{lo} neutrophils. In *a*, the spleen cells from 7-wk-old wild-type (WT) and *Xkr8*$^{-/-}$ C57BL/6 mice ($n = 5$ for each) were stained for CD62L and Gr1, and the FACS profiles for CD62L in the Gr1^{+} population are shown. In *Right* panels, the percentages of CD62L^{lo} neutrophils (indicated bars at *Left*), and the percentage caspase3/7-positive cells in CD62L^{hi} (hi) and CD62L^{lo} (lo) cells are plotted with the average value (bar). In *b*, G-CSF was injected into 10–14-wk-old wild-type and *Xkr8*$^{-/-}$ C57BL/6 mice ($n = 6$ for each) once a day, and 10 h after the third injection, the splenocytes were analyzed above. $^{*}P < 0.05$, $^{**}P < 0.01$, $^{***}P < 0.001$; two-sided Student's *t* test.

Masking PtdSer inhibits the efferocytosis of apoptotic thymocytes by peritoneal macrophages (27), and the loss of a PtdSer receptor (Tim4), PtdSer-binding proteins (Gas6 and Protein S), or TAM receptors (MerTK, Axl, and Tyro3) blocks efferocytosis (17, 28), together indicating that PtdSer exposure is indispensable for efferocytosis. During apoptosis, caspase cleaves and inactivates ATP11A and ATP11C, which normally flip PtdSer from the outer to inner leaflet of the plasma membrane (11, 12). Xkr8's scramblase activity is required for the PtdSer exposure and the efficient efferocytosis of apoptotic thymocytes, lymphocytes, and neutrophils, confirming that the PtdSer exposure by flippase inactivation alone is too slow for this process. Since the PtdSer exposed by Xkr8 scramblase can return to the inner layer by the flippase action of P4-ATPase, it is likely that both caspase-mediated activation of Xkr8 scramblase and inactivation of flippases are required for efferocytosis (26). How other molecules that have been proposed as "eat me" or "do not eat me" signals, including ICAM3, calreticulin, annexin, and CD47 (5, 29, 30) function in this process remains to be clarified.

Neutrophils have a short half life of about 12 h (31) and are programmed to undergo apoptosis (32). Although the trigger for neutrophil apoptosis in the aging process has not been elucidated, Bcl2-transgenic mice (33) and Noxa/Bim- or Bax/Bak double-deficient mice have twice the normal number of neutrophils in the circulation, indicating that the neutrophils' spontaneous apoptosis is mediated by the intrinsic mitochondrial death pathway (34, 35). We found that the number of CD62L^{lo} senescent neutrophils increased in the spleen of *Xkr8*-deficient mice, and some of them carried active caspase 3/7. These results indicate that, like apoptosis-induced neutrophils, caspase 3 is activated in senescent neutrophils and cleaves Xkr8 to elicit PtdSer exposure. It is likely that macrophages in the spleen, liver, and bone marrow engulf the senescent neutrophils in a PtdSer-dependent manner. In contrast to the increased number of senescent neutrophils in the spleen of *Xkr8*-deficient mice, the number in the blood was comparable to that in wild-type mice, which differs from mice carrying the disregulated Bcl-2 gene (34, 35). This observation may indicate that the Xkr8-mediated PtdSer exposure does not play a role in the migration of senescent neutrophils into the spleen. A caspase-dependent process is involved in recruiting macrophages to apoptotic cells (29); therefore, a similar caspase-dependent process may be involved in causing senescent neutrophils to approach macrophages in the spleen, liver, or bone marrow. In any case, *Xkr8*$^{-/-}$ mice, in particular after G-CSF treatment, accumulated a large amount of CD62L^{lo} neutrophils. This cell population will be useful for studies aimed at defining the so-far poorly characterized senescent neutrophils.

Similar to the knockout mice of other efferocytosis-related genes (MFG-E8, Tim4, and MerTK) (36–38), *Xkr8*-deficient mice on the MRL background showed high levels of anti-DNA antibodies and ANAs in the serum, activated effector T cells in the spleen, and IgG deposits in the glomeruli. It is likely that unengulfed apoptotic cells undergo secondary necrosis, releasing cellular contents including chromatin. Chromatin released from dying cells is a strong immunogen (39), but is normally cleaved by DNase1L3, a DNase I-like serum DNase (40). The MRL mouse strain carries a missense mutation in DNase1L3 that significantly reduces its DNase activity against chromatin (41). Thus, the chromatin released from unengulfed apoptotic cells due to inefficient efferocytosis may not be fully digested in this mouse strain. To confirm this possibility, it will be necessary to establish efferocytosis mutant mice on a DNase1L3-deficient C57BL/6 background. In any case, the treatment of patients with systemic lupus erythematosus (SLE) with G-CSF often causes severe flares (42). It is tempting to speculate that patients with SLE carry a defect in the efferocytosis system, and that overloading them with an increased number of apoptotic neutrophils worsens the disease.

The similar nephritis phenotype of mice deficient in *Xkr8*, *MFG-E8*, *Tim4*, and *MerTK* (36–38, 43) confirmed that these molecules are involved in the same process, PtdSer-dependent efferocytosis. MFG-E8 and Tim4 are expressed in different and limited subsets of macrophages (17, 44), while MerTK is expressed in almost all macrophages (44). Xkr8 is involved in the PtdSer exposure on apoptotic cells including senescent neutrophils. However, it is apparently not involved in the PtdSer exposure on pyrenocytes (nuclei expelled from erythroblasts) (45) or aged red blood cells (46), in which caspase(s) is apparently not activated. Pyrenocytes and aged red blood cells are still engulfed by macrophages in a PtdSer-dependent manner, in which MerTK and/or Tim4 may be involved. Thus, the severity of the SLE phenotype may differ among these knockout mice. In addition to lupus, the MFG-E8 deficiency causes dermatitis (47), and a worsened recovery after myocardial infarction due to the inefficient engulfment of apoptotic cells (48). It will be interesting to study whether the *Xkr8* deficiency causes similar phenotypes in the skin and heart, in particular in humans with the autoimmune disease.

Materials and Methods

Mice. C57BL/6J mice were purchased from Japan CLEA or Japan SLC. MRL/MpJ$^{+/+}$ mice were from Japan SLC. The *Xkr8*$^{-/-}$ mice on the C57BL/6 background are described in ref. 13. The MRL-*Xkr8*$^{-/-}$ mice were generated by backcrossing C57BL/6-*Xkr8*$^{-/-}$ mice to MRL/MPJ$^{+/+}$ mice using speed congenics (49). Genotyping with primers for a mouse marker set (49) indicated

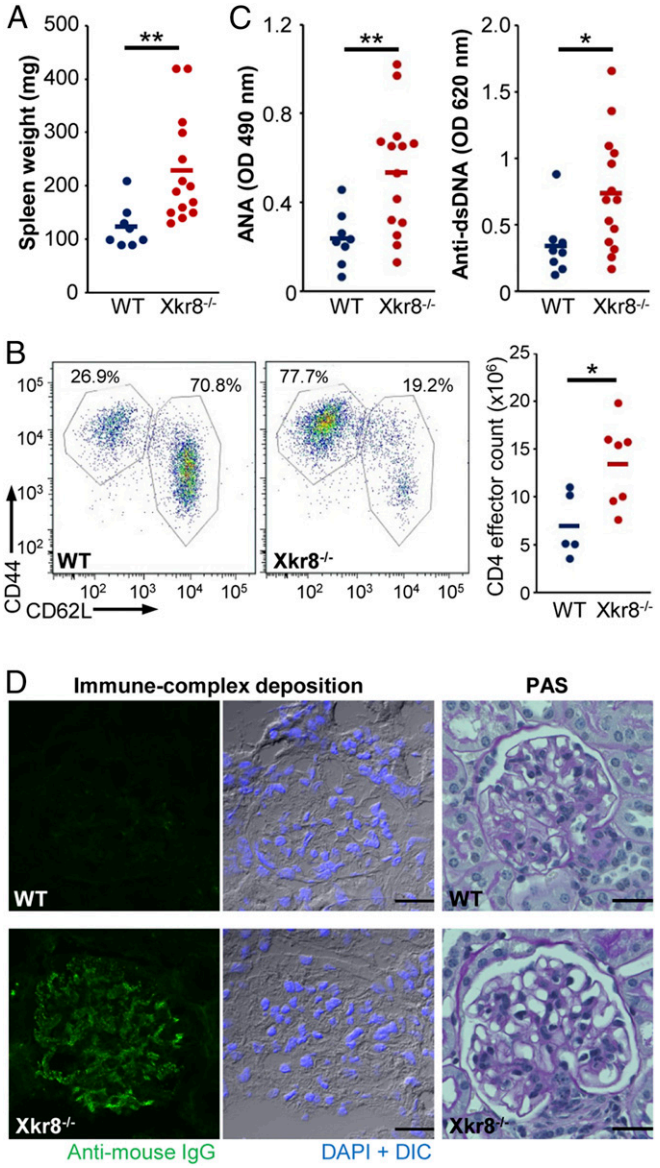

Fig. 5. Lupus-like response in female *Xkr8*$^{-/-}$ MRL mice. (*A*) Splenomegaly in *Xkr8*$^{-/-}$ mice. The weight of the spleen of 50-wk-old wild-type ($n = 8$) and *Xkr8*$^{-/-}$ ($n = 14$) mice (from seven litters) was plotted with the average value (bar). $^{**}P < 0.01$, two-sided Student's *t* test. (*B*) Accumulation of effector CD4^{+} T cells in the spleen of *Xkr8*$^{-/-}$ mice. The CD44^{hi}CD62L^{lo} effector and CD44^{lo}CD62L^{hi} naïve CD4 T cell populations are shown in a representative dot plot. *Right* shows the effector CD4 T cell count in 50-wk-old wild-type ($n = 5$) and littermate *Xkr8*$^{-/-}$ ($n = 7$) mice. $^{*}P < 0.05$, two-sided Student's *t* test. (*C*) Autoantibodies in serum. Sera were collected from 40-wk-old female wild-type ($n = 8$) or *Xkr8*$^{-/-}$ ($n = 14$) MRL mice (from seven litters), and the concentrations of ANA and anti-dsDNA antibodies were plotted with the average value (bar); $^{*}P < 0.05$; $^{**}P < 0.01$, two-sided Student's *t* test. (*D*) Development of glomerulonephritis. Kidney sections were prepared from 50-wk-old wild-type and *Xkr8*$^{-/-}$ mice. The sections were stained with PAS or with Alexa Fluor 488-conjugated anti-mouse IgG, followed by counterstaining with DAPI, and observed by fluorescence microscopy. (Scale bar, 20 μm.)

that the backcrossed mice had the MRL background at 98%. All mouse studies were approved by the Animal Care and Use Committee of the Research Institute of Microbial Diseases, Osaka University. All animals were maintained under specific pathogen-free conditions.

Cell Lines, Recombinant Proteins, and Antibodies. The *Axl*$^{-/-}$*Tyro3*$^{-/-}$*Gas6*$^{-/-}$NIH 3T3 cells expressing mouse Tim4 and MerTK (TKO-Tim4/Mer) (17) were cultured in DMEM containing 10% FCS. Human FasL was produced as described (50) and was partially purified by $(NH_4)_2SO_4$ precipitation at 60% saturation. Human G-CSF was provided by Chugai Pharmaceutical Co. Rat anti-mouse CD68 (clone FA-11) was from Bio-Rad. PE- or PE/Cy7-labeled anti-mGr1 (clone RB6-8C5), PE-anti-mCD3 (clone 145–2C11), FITC- or Brilliant Violet 510-labeled anti-mCD4 (clone RM4-5), PE/Cy7- or PerCP/Cy5.5-labeled anti-mCD8 (clone 53–6.7), APC-anti-mCD62L (clone MEL-14), and PE/Cy7-anti-mCD44 (clone IM7) mAbs were from BioLegend. Alexa Fluor 488-goat anti-mouse IgG and Alexa Fluor 594-goat anti-rat IgG were from Invitrogen. Horseradish peroxidase (HRP)-rabbit-anti-mouse Ig and alkaline phosphatase (AP)-rabbit anti-mouse Ig were from Dako.

Real-Time RT-PCR. RNA was reverse-transcribed using a High-Capacity RNA-to-cDNA kit (Applied Biosystems). Quantitative PCR was performed using the LightCycler 480 SYBR Green Master Mix (Roche Diagnostics) on a LightCycler 480 system. Plasmid DNA carrying the *Xkr* cDNA was linearized by digesting with a restriction enzyme and used as a reference. Primers used for PCR were: GAPDH, 5′-AACGACCCCTTCATTGAC-3′ and 5′-TCCAGACATACTCAGCAC-3′; Xkr4, 5′-GCCAGTGACCGTGATCAGAA-3′ and 5′-TCCTTGTACTGCAGCCTTGG-3′; Xkr8, 5′-GCGACGCCACACGCTCACACT-3′ and 5′-CCCCAGCAGCAGCAGGTTCC-3′; and Xkr9, 5′-GGAAGGCTGCCCGCAACTCA-3′ and 5′-TGGGCCAGAGTCCTCGGAGAA-3′.

Flow Cytometry and Apoptotic PtdSer Exposure. Cell suspensions were prepared from mouse spleen and thymus by squashing the tissue between glass slides. The cell suspensions were treated with RBC lysis solution (ACK Lysing Buffer; Thermo Fisher Scientific), filtered through nylon strainers, incubated with antibodies, and analyzed by flow cytometry (FACSCanto; BD Biosciences). In some cases, cells were incubated at 37 °C for 30 min with 1 μM CellEvent Caspase-3/7 Green (Thermo Fisher Scientific) before the flow cytometry. For TUNEL staining, cells were fixed at room temperature for 15 min in 2% paraformaldehyde (PFA), and permeabilized by incubating for 5 min in 0.1% Triton X-100. To prepare CD3^{+} splenocytes and Gr1^{+} blood neutrophils, splenocytes or blood leukocytes were obtained from 9-wk-old mice, stained with 0.5–1.0 μg/mL PE-anti-mouse CD3 or anti-Gr1 mAb, and sorted using a FACSAria II. The sorted CD3^{+} splenocytes (about 29% of the splenocytes) and Gr1^{+} neutrophils (about 9% of the blood leukocytes) were used for the efferocytosis assay.

To examine the apoptotic PtdSer exposure, thymocytes, splenocytes, or blood neutrophils were incubated at 37 °C for 0.5–3 h with 100 units/mL FasL or 10 μM ABT737 (Symantec). After washing with annexin V staining buffer [10 mM Hepes-NaOH buffer (pH 7.4), 140 mM NaCl, and 2.5 mM $CaCl_2$], the cells were stained on ice for 15 min with 1 μg/mL antibody for CD3, CD4, CD8, or Gr1, and 1,500-fold diluted Cy5-annexin V (Biovision) in annexin V staining buffer, and analyzed by flow cytometry using a FACSCanto.

Efferocytosis. Efferocytosis was carried out essentially as described previously in refs. 17 and 51. In brief, thymocytes and neutrophils were labeled with 0.1 μg/mL pHrodo Red, succinimidyl ester (Thermo Fisher Scientific), washed with PBS containing 10% FCS, and incubated at 37 °C with 100 units/mL FasL for 30 min (for thymocytes) or 1 h (for neutrophils) in DMEM containing 10% FCS. CD3^{+} splenocytes were similarly labeled with pHrodo, and incubated at 37 °C for 30 min with 10 μM ABT737 in DMEM containing 10% FCS. The pHrodo-labeled apoptotic cells were washed with DMEM containing 10% FCS, and used as prey. For efferocytosis, 1.5–2.4 × 10^{4} TKO-Tim4/Mer cells were cultured at 37 °C with the pHrodo-labeled prey in 0.3 mL of DMEM containing 10% FCS. After incubation, the cells were washed with PBS, and observed by confocal microscopy (FV1000, Olympus) in FluoroBrite DMEM (Thermo Fischer Scientific) containing 10% FCS.

Treatment with Dexamethasone, G-CSF, or Zymosan. Dexamethasone (Wako Pure Chemical) was i.p. administered to 6- to 9-wk-old mice at a dose of 8 mg/kg. The thymuses were harvested 12 h after the injection for histological analysis. Human G-CSF was s.c. injected into mice at a dose of 2.5 μg per mouse, and the spleens were harvested for flow cytometry analysis with PE/Cy7-labeled anti-Gr1 and APC-labeled anti-CD62L. Zymosan-induced peritonitis was performed essentially as described (52). In brief, mice at 6–8 wk of age were injected i.p. with zymosan A particles (250 mg/kg, 0.5 mL saline; Sigma-Aldrich). Cells in the peritoneal lavage fluid were harvested with 5 mL PBS containing 2% FCS at 18 h after the injection, counted, and subjected to the flow cytometry analysis for Gr1^{+} neutrophils as described above.

Histochemical Analysis. For periodic acid Schiff (PAS) staining, tissues were fixed at 4 °C overnight with 4% PFA in PBS, embedded in paraffin, sectioned at 3 μm, and stained at room temperature for 30 min with Schiff's reagent (Merck). To detect the immune-complex deposition in glomeruli, fresh kidneys were embedded in optimal cutting temperature (OCT) compound

(Sakura Finetek), sectioned at 6 μm, and fixed with cold acetone. After blocking nonspecific sites by incubating at room temperature for 1 h in PBS containing 5% goat serum (Invitrogen), the sections were stained for 1 h with Alexa Fluor 488-goat anti-mouse IgG. For TUNEL staining, the thymus was fixed at 4 °C overnight with 4% PFA in PBS, embedded in OCT compound, and sectioned at 6 μm. TUNEL staining was performed using the Apoptag In situ Apoptosis Detection kit (Merck Millipore) according to the instructions provided by the supplier. The stained sections were mounted with Fluoromount (Diagnostic Biosystems) and observed by fluorescence microscopy (BioRevo BZ-9000, Keyence).

Measurements of Autoantibodies in Serum. The serum level of anti-dsDNA antibodies and ANAs were quantified essentially as described (27). In brief, linearized plasmid DNA (5 μg/mL) was immobilized to NucleoLink plates (Nunc) by treatment with 10 mM 1-ethyl-3-(3-dimethylaminopropyl)-carbodiimidide (Sigma-Aldrich) in 10 mM 1-methylimidazole (Sigma-Aldrich) at 50 °C for 5 h. After washing with 5× saline-sodium citrate (SSC) (150 mM NaCl, 15 mM trisodium citrate, pH 7.0) containing 0.25% SDS, nonspecific binding sites on the DNA-coated plates were blocked by incubation with 1% BSA in PBS (blocking buffer) at 4 °C overnight. Mouse sera were diluted 100 times with the blocking buffer, and 100-μL aliquots were applied to the DNA-coated plates and incubated for 1 h at room temperature. After washing with PBS containing 0.1% Tween 20, the bound antibodies were detected using AP-conjugated rabbit anti-mouse Ig and the BluePhos Microwell Phosphatase Substrate system, and quantified by measuring the absorbance at 620 nm. The ANA level was determined using a Mesacup EIA system [Medical Biological Laboratories (MBL)] for human ANA, except that the HRP-conjugated anti-human Ig was replaced with HRP-conjugated rabbit anti-mouse Ig.

ACKNOWLEDGMENTS. We thank Dr. J. Suzuki and Mr. E. Imanishi for the initial stage of this project and Ms. M. Fujii for secretarial assistance. This work was supported in part by Grants-in-Aid for Specially Promoted Research from the Japan Society for the Promotion of Science (15H05785) and from Core Research for Evolutional Science and Technology, Japan Science and Technology Agency (JPMJCR14M4). M.K. is a Research Fellow of the Japan Society for the Promotion of Science.

1. Fuchs Y, Steller H (2011) Programmed cell death in animal development and disease. *Cell* 147:742–758.
2. Crawford ED, Wells JA (2011) Caspase substrates and cellular remodeling. *Annu Rev Biochem* 80:1055–1087.
3. Wallach D, Kang TB, Dillon CP, Green DR (2016) Programmed necrosis in inflammation: Toward identification of the effector molecules. *Science* 352:aaf2154.
4. Kumar S, Calianese D, Birge RB (2017) Efferocytosis of dying cells differentially modulate immunological outcomes in tumor microenvironment. *Immunol Rev* 280: 149–164.
5. Nagata S, Apoptosis and the clearance of apoptotic cells. *Annu Rev Immunol*, 10.1146/annurev-immunol-042617-053010.
6. Muñoz LE, Lauber K, Schiller M, Manfredi AA, Herrmann M (2010) The role of defective clearance of apoptotic cells in systemic autoimmunity. *Nat Rev Rheumatol* 6: 280–289.
7. Ren Y, Savill J (1998) Apoptosis: The importance of being eaten. *Cell Death Differ* 5: 563–568.
8. Savill J, Dransfield I, Gregory C, Haslett C (2002) A blast from the past: Clearance of apoptotic cells regulates immune responses. *Nat Rev Immunol* 2:965–975.
9. Leventis PA, Grinstein S (2010) The distribution and function of phosphatidylserine in cellular membranes. *Annu Rev Biophys* 39:407–427.
10. Bevers EM, Williamson PL (2016) Getting to the outer leaflet: Physiology of phosphatidylserine exposure at the plasma membrane. *Physiol Rev* 96:605–645.
11. Segawa K, Kurata S, Nagata S (2016) Human type IV P-type ATPases that work as plasma membrane phospholipid flippases, and their regulation by caspase and calcium. *J Biol Chem* 291:762–772.
12. Segawa K, et al. (2014) Caspase-mediated cleavage of phospholipid flippase for apoptotic phosphatidylserine exposure. *Science* 344:1164–1168.
13. Suzuki J, Denning DP, Imanishi E, Horvitz HR, Nagata S (2013) Xk-related protein 8 and CED-8 promote phosphatidylserine exposure in apoptotic cells. *Science* 341: 403–406.
14. Suzuki J, Imanishi E, Nagata S (2014) Exposure of phosphatidylserine by Xk-related protein family members during apoptosis. *J Biol Chem* 289:30257–30267.
15. Suzuki J, Imanishi E, Nagata S (2016) Xkr8 phospholipid scrambling complex in apoptotic phosphatidylserine exposure. *Proc Natl Acad Sci USA* 113:9509–9514.
16. van Delft MF, et al. (2006) The BH3 mimetic ABT-737 targets selective Bcl-2 proteins and efficiently induces apoptosis via Bak/Bax if Mcl-1 is neutralized. *Cancer Cell* 10: 389–399.
17. Yanagihashi Y, Segawa K, Maeda R, Nabeshima YI, Nagata S (2017) Mouse macrophages show different requirements for phosphatidylserine receptor Tim4 in efferocytosis. *Proc Natl Acad Sci USA* 114:8800–8805.
18. Surh CD, Sprent J (1994) T-cell apoptosis detected *in situ* during positive and negative selection in the thymus. *Nature* 372:100–103.
19. Loo DT (2010) *In Situ Detection of Apoptosis by the TUNEL Assay: An Overview of Techniques* (Humana Press, Totowa, NJ), Vol 682, pp 3–13.
20. Greenlee-Wacker MC (2016) Clearance of apoptotic neutrophils and resolution of inflammation. *Immunol Rev* 273:357–370.
21. Kolaczkowska E, Koziol A, Plytycz B, Arnold B (2010) Inflammatory macrophages, and not only neutrophils, die by apoptosis during acute peritonitis. *Immunobiology* 215: 492–504.
22. Casanova-Acebes M, et al. (2013) Rhythmic modulation of the hematopoietic niche through neutrophil clearance. *Cell* 153:1025–1035.
23. Strydom N, Rankin SM (2013) Regulation of circulating neutrophil numbers under homeostasis and in disease. *J Innate Immun* 5:304–314.
24. Vratsanos GS, Jung S, Park YM, Craft J (2001) CD4(+) T cells from lupus-prone mice are hyperresponsive to T cell receptor engagement with low and high affinity peptide antigens: A model to explain spontaneous T cell activation in lupus. *J Exp Med* 193: 329–337.
25. Rankin AL, et al. (2012) IL-21 receptor is required for the systemic accumulation of activated B and T lymphocytes in MRL/MpJ-Fas(lpr/lpr)/J mice. *J Immunol* 188: 1656–1667.
26. Nagata S, Suzuki J, Segawa K, Fujii T (2016) Exposure of phosphatidylserine on the cell surface. *Cell Death Differ* 23:952–961.
27. Asano K, et al. (2004) Masking of phosphatidylserine inhibits apoptotic cell engulfment and induces autoantibody production in mice. *J Exp Med* 200:459–467.
28. Lew ED, et al. (2014) Differential TAM receptor-ligand-phospholipid interactions delimit differential TAM bioactivities. *eLife* 3:e03385.
29. Medina CB, Ravichandran KS (2016) Do not let death do us part: 'Find-me' signals in communication between dying cells and the phagocytes. *Cell Death Differ* 23:979–989.
30. Henson PM (2017) Cell removal: Efferocytosis. *Annu Rev Cell Dev Biol* 33:127–144.
31. Basu S, Hodgson G, Katz M, Dunn AR (2002) Evaluation of role of G-CSF in the production, survival, and release of neutrophils from bone marrow into circulation. *Blood* 100:854–861.
32. Williams GT, Smith CA, Spooncer E, Dexter TM, Taylor DR (1990) Haemopoietic colony stimulating factors promote cell survival by suppressing apoptosis. *Nature* 343:76–79.
33. Ogilvy S, et al. (1999) Constitutive Bcl-2 expression throughout the hematopoietic compartment affects multiple lineages and enhances progenitor cell survival. *Proc Natl Acad Sci USA* 96:14943–14948.
34. Geering B, Simon H-U (2011) Peculiarities of cell death mechanisms in neutrophils. *Cell Death Differ* 18:1457–1469.
35. Kirschnek S, et al. (2011) Molecular analysis of neutrophil spontaneous apoptosis reveals a strong role for the pro-apoptotic BH3-only protein Noxa. *Cell Death Differ* 18:1805–1814.
36. Hanayama R, et al. (2004) Autoimmune disease and impaired uptake of apoptotic cells in MFG-E8-deficient mice. *Science* 304:1147–1150.
37. Rodriguez-Manzanet R, et al. (2010) T and B cell hyperactivity and autoimmunity associated with niche-specific defects in apoptotic body clearance in TIM-4-deficient mice. *Proc Natl Acad Sci USA* 107:8706–8711.
38. Cohen PL, et al. (2002) Delayed apoptotic cell clearance and lupus-like autoimmunity in mice lacking the c-mer membrane tyrosine kinase. *J Exp Med* 196:135–140.
39. Burlingame RW, Boey ML, Starkebaum G, Rubin RL (1994) The central role of chromatin in autoimmune responses to histones and DNA in systemic lupus erythematosus. *J Clin Invest* 94:184–192.
40. Sisirak V, et al. (2016) Digestion of chromatin in apoptotic cell microparticles prevents autoimmunity. *Cell* 166:88–101.
41. Wilber A, O'Connor TP, Lu ML, Karimi A, Schneider MC (2003) Dnase1l3 deficiency in lupus-prone MRL and NZB/W F1 mice. *Clin Exp Immunol* 134:46–52.
42. Starkebaum G (2002) Chronic neutropenia associated with autoimmune disease. *Semin Hematol* 39:121–127.
43. Khan TN, Wong EB, Soni C, Rahman ZSM (2013) Prolonged apoptotic cell accumulation in germinal centers of Mer-deficient mice causes elevated B cell and CD4+ Th cell responses leading to autoantibody production. *J Immunol* 190:1433–1446.
44. Summers KM, Hume DA (2017) Identification of the macrophage-specific promoter signature in FANTOM5 mouse embryo developmental time course data. *J Leukoc Biol* 102:1081–1092.
45. Yoshida H, et al. (2005) Phosphatidylserine-dependent engulfment by macrophages of nuclei from erythroid precursor cells. *Nature* 437:754–758.
46. Lutz HU, Bogdanova A (2013) Mechanisms tagging senescent red blood cells for clearance in healthy humans. *Front Physiol* 4:387.
47. Peng Y, Elkon KB (2011) Autoimmunity in MFG-E8-deficient mice is associated with altered trafficking and enhanced cross-presentation of apoptotic cell antigens. *J Clin Invest* 121:2221–2241.
48. Nakaya M, et al. (2017) Cardiac myofibroblast engulfment of dead cells facilitates recovery after myocardial infarction. *J Clin Invest* 127:383–401.
49. Wakeland E, Morel L, Achey K, Yui M, Longmate J (1997) Speed congenics: A classic technique in the fast lane (relatively speaking). *Immunol Today* 18:472–477.
50. Shiraishi T, et al. (2004) Increased cytotoxicity of soluble Fas ligand by fusing isoleucine zipper motif. *Biochem Biophys Res Commun* 322:197–202.
51. Toda S, Hanayama R, Nagata S (2012) Two-step engulfment of apoptotic cells. *Mol Cell Biol* 32:118–125.
52. Cash JL, White GE, Greaves DR (2009) Chapter 17. Zymosan-induced peritonitis as a simple experimental system for the study of inflammation. *Methods Enzymol* 461: 379–396.